

Magnetoresistance in terbium and holmium single crystals*

R. L. Singh, M. H. Jericho, and D. J. W. Geldart

Department of Physics, Dalhousie University, Halifax, Nova Scotia, Canada B3H 3J5

(Received 18 August 1975)

The longitudinal magnetoresistance of single crystals of terbium and holmium metals in their low-temperature ferromagnetic phase has been investigated in magnetic fields up to 80 kOe. Typical magnetoresistance isotherms exhibit a minimum which increases in depth and moves to higher fields as the temperature increases. The magnetoresistance around 1 K, where inelastic scattering is negligible, has been interpreted as the sum of a negative contribution due to changes in the domain structure and a positive contribution due to normal magnetoresistance. At higher temperatures, a phenomenological approach has been developed to extract the inelastic phonon and spin-wave components from the total measured magnetoresistance. In the temperature range 4–20 K (approximately), the phonon resistivity varies as $T^{3.7}$ for all samples. Approximate upper and lower bounds have been placed on the spin-wave resistivity which is also found to be described by a simple power law in this temperature range. The implications of this result for theoretical treatments of spin-wave resistivity due to s - f exchange interactions are considered. It is concluded that the role played by the magnon energy gap is far less transparent than previously suggested.

I. INTRODUCTION

The magnetic properties of the heavy-rare-earth metals are associated with the distribution of $4f$ electrons localized in the ionic cores. The s - f exchange interaction between the itinerant conduction electrons and the localized ionic spins gives rise to a spin-dependent contribution to resistivity, ρ_s , which depends on the degree of ordering of the localized ionic spins. The detailed behavior of ρ_s , particularly in the vicinity of a magnetic-ordering temperature, is not completely understood at present. Sufficiently far above the upper magnetic-ordering temperature, the ionic spins are randomly oriented. In this spin-disorder limit, Kasuya¹ and de Gennes and Friedel² showed that ρ_s tends to a constant value given by $\rho_{dis} \propto (g-1)^2 J(J+1)$, where g is the Landé factor and J is the total ionic angular momentum divided by \hbar . A good correlation between the de Gennes factor $(g-1)^2 J(J+1)$ and the measured ρ_{dis} has been experimentally observed across the heavy-rare-earth series.³

The low-temperature ferromagnetic state should also be relatively simple, in principle, since correlations between the ionic spins should be then adequately described by a one-magnon approximation. Unfortunately, this regime is still not well understood. Theoretical attempts to describe ρ_s in the low-temperature state of these metals have been rather limited. Also, experimental estimates of the spin-wave resistivity are ambiguous due to the difficulty of isolating ρ_s from contributions due to inelastic electron-phonon scattering. In an earlier work,⁴ the phonon resistivity was taken to be described by the Bloch T^5 law. Although this

method may be adequate for some simple monovalent metals, it is inadequate for complex polyvalent metals such as the rare earths. In the present work we have made an effort to isolate the low-temperature spin-wave resistivity in Tb and Ho single crystals without presupposing any explicit expression for the phonon resistivity. Our approach is based on the fact that high magnetic fields suppress magnon excitations; consequently, electron-magnon scattering and ρ_s can be suppressed. Thus, it should be possible to extract the spin-wave resistivity from magnetoresistance data. Some high-field magnetoresistance results on polycrystalline Gd have been reported by Lüthi and Rohrer.⁵ We report here detailed magnetoresistance results on Tb and Ho single crystals. The outline of the paper is as follows.

In Sec. II, we give experimental details about the sample preparation and the measurement techniques. The magnetoresistance results are given in Sec. III. A phenomenological approach to isolate the spin-wave resistivity from the data is described in Sec. IV and the temperature dependence of the spin-wave and the phonon resistivities is discussed. Finally, the implications of these results are considered in Sec. V, with particular emphasis on the problem of obtaining information about the magnon energy gap from the spin-wave resistivity.

II. EXPERIMENTAL DETAILS

The samples were prepared from two single crystals of Tb and Ho which were purchased from Metals Research Co., Limited. The stated purity was 99.9% and typical impurity analysis for both

samples showed 1000 ppm wt. (max.) of other rare earths and trace amounts of Ta and W and other metals present in amounts not exceeding 200 ppm wt. (max.). It is probable that the major impurity present was oxygen.⁶ The various resistivity samples were spark cut from these larger crystals. The sample axis was aligned with a particular crystallographic direction to within about 1°. Typical sample dimensions were $4 \times 0.5 \times 0.5$ mm³. After cutting and subsequent cleaning, the samples were annealed at 600 °C for 6–8 h in previously degassed quartz tubes at a pressure of 3×10^{-7} torr. Electrical contact was made through fine platinum leads spot welded to each sample. The potential leads were attached as far away from the current contacts as possible in order to reduce end effects. The above procedure resulted in resistance ratios $[R(300)/R(4.2)]$ of between 20 and 25 for all samples. At 4 K the resistivities were about 7 and 4 $\mu\Omega$ cm for the Tb and Ho crystals, respectively. Some specimens were annealed at 800 °C without significant change in their resistance ratio.

The samples were attached to copper blocks with varnish. The blocks in turn were coated with tissue paper and GE varnish to isolate the samples electrically. These copper blocks were then mounted on the main body of the sample holder which carried the various thermometers. The samples were mounted with the current direction either parallel or perpendicular to the magnetic field with an alignment error of not more than $9 \pm 3^\circ$. Repeated measurements on the same sample showed that slowly cooled specimens had lower resistances at 4 K than when cooled rapidly. It is most likely that the above method of mounting the sample introduces strains so that the rapidly cooled specimens were relatively more strained than the slowly cooled samples. The magnetoresistance results should not, however, be significantly affected by this small amount of extra resistance. All electrical leads to the sample were anchored to the sample mount assembly to eliminate lead movement in the magnetic field.

The resistance variations with field and temperature were measured with an ac potentiometer technique which will be described elsewhere.⁷ Basically, the potential across the sample is compared with that across a reference resistor kept at room temperature. The currents through the sample and reference resistors are chopped synchronously via two electronic switches and the unbalance signal is detected with a lock-in amplifier. The current ratio through the two circuits is then measured with two voltage-to-frequency converters and it is directly proportional to the sample resistance with a precision of one part in 20 000 and better. Because of the uncertainty in the sample

shape factor, the experimental results are given in terms of this current ratio. As a check on this ac method of measuring the magnetoresistance we examined specimens of Cu and Fe both at room temperature and helium temperature and compared the photochopper results with results obtained with a conventional dc potentiometer and galvanometer amplifier arrangement. In both cases the two sets of results agreed to within one part in 10^4 .

Three temperature sensors were used. A calibrated germanium thermometer (Cryo Cal Inc.) served as primary thermometer. To avoid effects of the magnetic field on the temperature sensor we employed a capacitance thermometer to measure temperatures when the field was on. The capacitance thermometer had a sensitivity of 200 pF/K near 4 K and the capacitance was measured with a General Radio Co. type 1615-A capacitance bridge with a resolution of 0.2 pF at a frequency of 5 kHz. The bridge null was measured with a lock-in amplifier and the output of the lock-in was used as input signal for a temperature controller which controlled the current through a heater in direct contact with the sample mount. Between 4 and 25 K the temperature stability in fields up to 85 kOe was about ± 10 mK. For temperatures near 60 K stabilization was achieved via a copper-constantan thermocouple rather than the capacitance sensor.

III. RESULTS

Before we present the actual magnetoresistance data we would like to make a few general comments concerning the dependence of resistivity on the samples' initial magnetic state.

The resistance measurements on several Tb and Ho samples show that (i) the resistance well below the ordering temperature depends on the cooling rate of the specimens from room temperature down to 4.2 K, as mentioned in Sec. II, and (ii) the magnetoresistance isotherms show a hysteresis effect. The first effect, although it will determine in part the actual resistivity of the samples at low temperatures, did not, however, affect the magnetoresistance results. In an attempt to check effects of thermal hysteresis on the isotherms several runs were made on the *b*-axis crystal using different cooling rates. In one run the sample was cooled down from room temperature to helium temperature within 4 h. In another run the cooling time from room temperature down to 100 K was 24 h, and from this temperature down to 4.2 K was about 2 h. At 1.2 K, the sample resistance in these two runs differed by almost 3%. In every case, slowly cooled samples produced lower resistances. However, the major features of the re-

sults, such as depth of the resistance minimum and its dependence on temperature (see below), were independent of the cooling rate to within the experimental error. Furthermore, the magnetic field at the minimum was also found to be independent of the thermal cycling. The cause of this resistance variation is most likely due to strain introduced in the specimens during cooling.

In the second effect, as the magnetic field is applied at a given temperature, the resistance changes and, on reducing the field back to zero, the resistance does not return to its virgin-state value (i.e., unmagnetized state) but to a lower value which depends on the sample material and its crystal orientation. On subsequent field cycling, the resistance always returns to this lower value. At 1.2 K these decreases in the resistance are 2.2% and 1.6% for the Tb *b*- and *a*-axis crystals, respectively, and the corresponding changes for the Ho crystals are 4.1% and 2.1%. We attribute this resistance decrease to magnetic-domain realignment in the crystals. Thus, after magnetization, samples seem to have fewer domains than in the virgin state, and a common procedure is, therefore, required to define a standard initial magnetic state so that meaningful comparison can be made of different resistance isotherms. The following procedure was adopted for all measurements reported in this paper.

First, the sample resistance as a function of temperature was measured from 1.2 to 35 K. It was then cooled down again to 4.2 K and magnetoresistance isotherms were taken both for increasing and decreasing field, and *H* parallel or antiparallel to the sample current. For *H* > 10 kOe the results were independent of the four field orientations, but at lower fields the resistivity showed a hysteresis effect. When the direction of the magnetizing field was reversed, the isotherm passed through a small maximum (0.2%) at around $\frac{1}{2}$ kOe. Finally, the sample was cooled down to 1.2 K and data for the resistance versus field were taken for one direction of the field only.

A. Resistance results for Tb crystals

The longitudinal magnetoresistance isotherms for a Tb $\langle 10\bar{1}0 \rangle$ -axis crystal are shown in Fig. 1. The resistance initially decreases as the magnetic field increases and finally passes through a minimum. The increase in the resistance at higher fields is very similar to that observed in nonmagnetic metals. The depth of the resistance minimum and its position are both temperature dependent. The depth of the resistance minimum is measured relative to the zero-field value and is 2.48% of the zero-field value at 1.22 K and rises to

3.92% at 22.6 K. For the above two isotherms, the minimum appears at around 1.4 and 8.0 kOe, respectively. Some of the resistance versus magnetic field curves for a Tb $\langle 11\bar{2}0 \rangle$ -axis crystal are shown in Fig. 2. The qualitative behavior of these results is very similar to the *b*-axis results. However, the rate of decrease of the resistance in this case is lower and as a consequence the minimum appears at higher fields. For example, at 1.19 K the minimum occurs around 5.6 kOe. A slow decrease in the resistance is due to the basal-plane magnetic anisotropy which does not favor domain alignment parallel to the *a* axis. The depth of the minimum is 5.1% at 1.19 K and rises to more than 8.0% at 31.3K.

B. Resistivity results for Ho crystals

Figure 3 shows some of the longitudinal magnetoresistance isotherms for a Ho $\langle 10\bar{1}0 \rangle$ -axis crystal. The resistance minimum at 1.19 K occurs around 4 kOe and at 14.4 K it moves to 75 kOe.

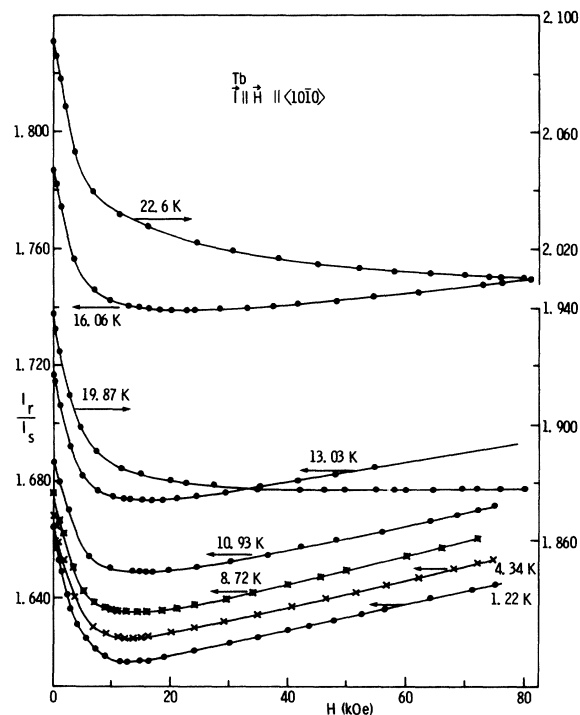


FIG. 1. Variation of the longitudinal magnetoresistance as a function of the applied field for the Tb $\langle 10\bar{1}0 \rangle$ axis crystal with sample current $\vec{I} \parallel \vec{H} \parallel \langle 10\bar{1}0 \rangle$. I_r/I_s is the ratio of the currents in the reference and the sample resistance is equal to the product of this ratio and the reference resistance which is a constant. The changes in the depth of the resistance minimum are due to reduction in the electron-spin-wave scattering.

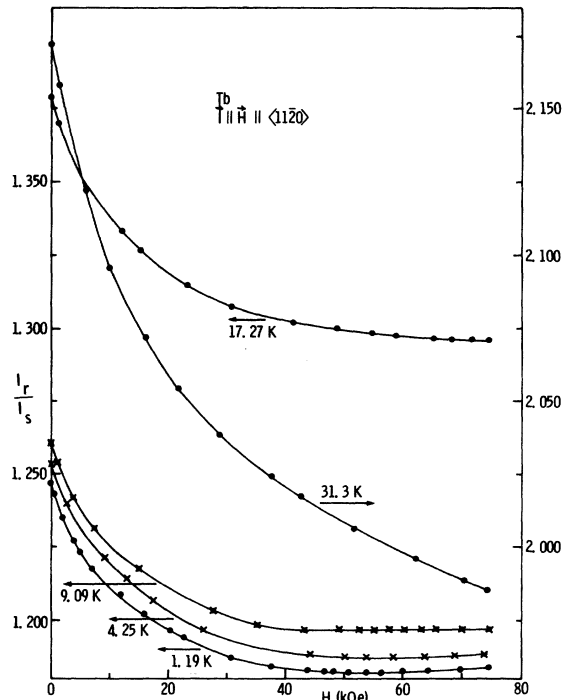


FIG. 2. Variation of the longitudinal magnetoresistance as a function of the applied field for the Tb $\langle 11\bar{2}0 \rangle$ axis crystal. Sample current $\bar{I} \parallel \bar{H} \parallel \langle 11\bar{2}0 \rangle$.

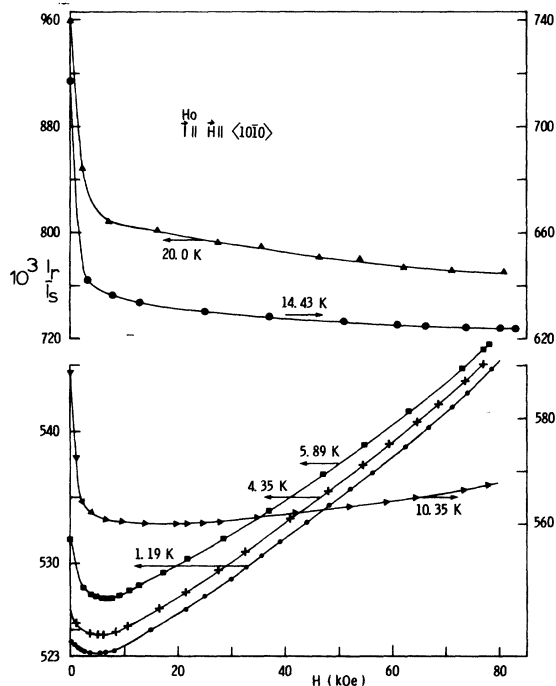


FIG. 3. Variation of the longitudinal magnetoresistance as a function of the applied field for the Ho $\langle 10\bar{1}0 \rangle$ axis crystal. Sample current $\bar{I} \parallel \bar{H} \parallel \langle 10\bar{1}0 \rangle$.

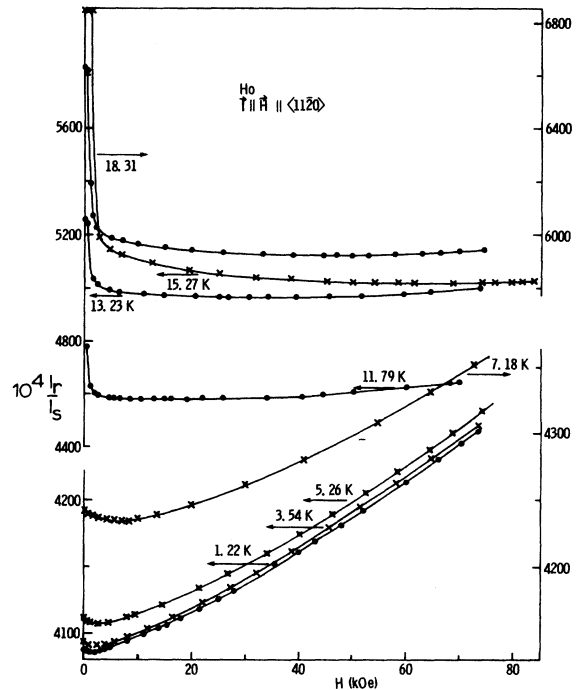


FIG. 4. Variation of the longitudinal magnetoresistance as a function of the applied field for the Ho $\langle 11\bar{2}0 \rangle$ axis crystal. Sample current $\bar{I} \parallel \bar{H} \parallel \langle 11\bar{2}0 \rangle$.

The depth of the minimum with respect to the zero-field resistance increases from 0.26% to 11.6% for the above temperatures. Some of the magnetoresistance isotherms for a Ho $\langle 11\bar{2}0 \rangle$ -axis crystal are shown in Fig. 4. The qualitative behavior of these results is very similar to that of the b -axis crystal.

IV. ANALYSIS OF THE RESISTIVITY RESULTS

The total resistivity is generally expressed as the sum of various resistivity components and for a magnetic metal can be written as

$$\rho = \rho_r + \rho_p + \rho_D + \rho_S, \quad (1)$$

where ρ_r is the resistivity due to impurities and static lattice imperfections, ρ_p is the resistivity due to phonons, ρ_D is the contribution associated with magnetic domains, and ρ_S is the resistivity due to spin waves. The sum of ρ_r and ρ_p is the nonmagnetic part of the resistivity, while ρ_D and ρ_S are expected to be strongly dependent on the applied magnetic field. The determination of the field and temperature dependence of the various components is a formidable problem.⁸ Since no trustworthy comprehensive theory exists as yet for the electrical resistivity of complex magnetic metals, we are obliged to adopt a phenomenological approach.

The essential point is that the temperature-dependent resistivity due to inelastic scattering, $\rho_p + \rho_s$, is imposed on a magnetic-field-dependent background which must be extracted from the total resistivity data if we are to accomplish our objective of isolating the magnon-induced contribution. The general features of this background are apparent from the $T=1.2$ K isotherm in Fig. 1, where the inelastic contribution is negligible. The magnetoresistance at $T=1.2$ K can be interpreted as the sum of a rapidly varying negative contribution, which saturates at relatively low fields, and a slowly varying positive contribution which dominates in the high-field region. The negative contribution is ascribed to domain effects (wall motion, domain reorientation, etc.) which is supported by the fact that it saturates at fields where technical saturation of the magnetization occurs.^{9,10} The slowly varying positive contribution is characteristic of the normal magnetoresistance, owing to the Lorentz force on the conduction electrons, which is observed for nonmagnetic metals as well as for the 3d-transition-series ferromagnets.¹¹

At higher temperatures, there are temperature-dependent contributions to the resistivity due to inelastic scattering of electrons from phonons and spin waves. In addition, the purely "elastic" background magnetoresistance, due to domain and Lorentz-force effects, may be temperature dependent. In the following analysis, we assume that this implicit temperature dependence of the background can be neglected relative to that arising from the explicit inelastic scattering. The reasons are the following: (i) The domain structure and stabilization at low temperature are determined primarily by static imperfections, which are not temperature dependent, and by magnetic and other anisotropy energies. The temperature dependence of the latter enters implicitly through the spontaneous magnetization which is field dependent but is certainly not strongly temperature dependent^{9,10} in the range of present interest ($T \lesssim 30$ K). (ii) To appreciate the fact that the temperature dependence of the normal magnetoresistance is also weak, suppose that it may be represented by a form of Kohler's rule,¹² appropriately modified for a ferromagnet, $\Delta\rho(T, B)/\rho(T, 0) = F(B/\rho(T, 0))$. The temperature dependence of $B = H + 4\pi M$ is weak, as discussed above. The determination of $\rho(T, 0)$ is delicate for high-purity materials,^{11,13,14} but the low-field resistivity of the present rare-earth-metal samples is dominated by the residual resistivity (due to static imperfections such as impurities) throughout the temperature range of interest. Consequently, we may set $\rho(T, 0) \approx \rho_r$ to a good first approximation¹⁵ so that the dominant contribution to the normal magneto-

resistance is seen to be also weakly temperature dependent.

As a result of these considerations, we conclude that the temperature dependence of $\rho(T, H)$ is dominated by inelastic scattering from phonons and magnons. Thus, the net contribution of inelastic scattering, for a given applied field H , may then be extracted from the total resistivity by simply subtracting the field-dependent, but temperature-independent, elastic background which is given by $\rho(T=1.2 \text{ K}, H)$. That is, $\rho(T, H) - \rho(1.2 \text{ K}, H) = \rho_{\text{inel}}(T, H)$ is to be interpreted as the sum of a phonon contribution ρ_p , which is very weakly field dependent, and a spin-wave contribution ρ_s . The latter is not only temperature dependent but is also field dependent due to suppression of thermal magnons by an applied field. The validity of this interpretation is illustrated by Fig. 5(a) where we have plotted $\rho_{\text{inel}}(T, H)$ for a Ho b -axis crystal as a function of temperature for applied fields of $H=0, 8, 80$ kOe. As expected, $\rho_{\text{inel}}(T, H)$ is a monotone-

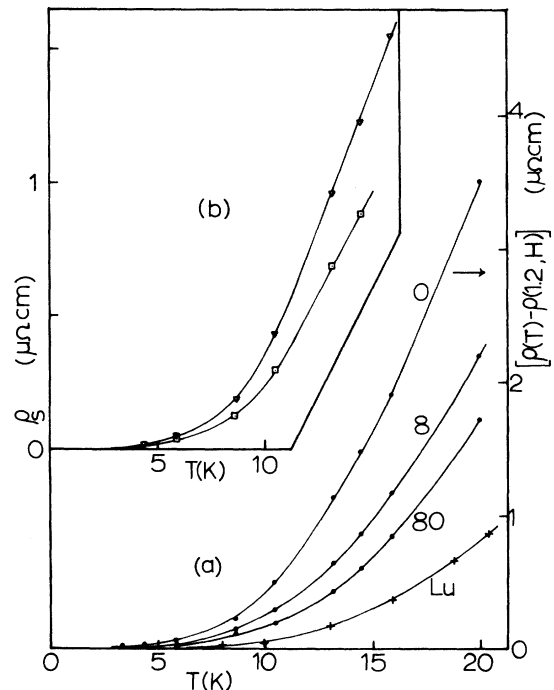


FIG. 5. (a) Temperature variation of the inelastic resistivity $\rho_{\text{inel}}^{\text{Ho}}(T, H)$ for Ho b -axis crystal for fields of 0, 8, and 80 kOe. Also shown is the zero-field inelastic resistivity $\rho_{\text{inel}}^{\text{Lu}}(T)$ of a b -axis Lu crystal (Ref. 17). (b) ∇ —magnon resistivity obtained by subtracting $\rho_{\text{inel}}^{\text{Lu}}(T)$ from $\rho_{\text{inel}}^{\text{Ho}}(T, H)$. This represents an upper limit to $\rho_{\text{inel}}^{\text{Ho}}(T, H)$. \square —magnon resistivity of b -axis Ho from Eq. (4) and the assumption that all magnons are quenched in a field of 80 kOe. This represents a lower limit to $\rho_{\text{inel}}^{\text{Ho}}(T, H)$.

nically increasing function of T and a decreasing function of H . The determination of $\rho_s(T, H)$ from Fig. 5(a) is still not trivial since $\rho_p(T)$ is not known *a priori* for Ho. However, it is reasonable to expect the phonon resistivities of Ho and non-magnetic Lu to be quite similar (their Debye temperatures^{16,18} are 161 and 165 K, respectively). The temperature-dependent contribution to the resistivity of a b -axis crystal of Lu, as given by Boys,¹⁹ is also given in Fig. 5. If we assume $\rho_{\text{inel}}^{\text{Lu}}(T)$ to be an adequate approximation to $\rho_p^{\text{Ho}}(T)$, then the purely magnon contribution to Ho resistivity is given by

$$\rho_s^{\text{Ho}}(T, H) \approx \rho_{\text{inel}}^{\text{Ho}}(T, H) - \rho_{\text{inel}}^{\text{Lu}}(T).$$

The magnon resistivity determined in this way is shown as the upper curve in Fig. 5(b) for the zero-field case.

It is clear from Fig. 5 that the temperature dependence (monotonically increasing) and the field dependence (monotonically decreasing) of $\rho_s(T, H)$ are qualitatively as expected. Of course, this estimate of ρ_s is based on the assumption that the phonon-induced resistivities of Ho and Lu are very similar. Although this assumption is not unreasonable, it is useful to have a second and independent method for estimating ρ_s . An alternative approach will therefore be given.

The magnetoresistance data are first corrected for the effect of magnetostriction on the sample shape factor,⁸ and the corrected magnetoresistance $R^*(T, H)$ is expressed in dimensionless form as $R^*(T, H)/R_0 = \rho(T, H)/\rho_0$, where R_0 is the sample resistance at $T = 1.2$ K and $H = 0$. Based on the previously discussed picture of field-dependent contributions due to domain and Lorentz-force effects, the $T = 1.2$ K isotherm was characterized by

$$\rho(1.2\text{K}, H) = \rho_r + \rho_D(H) + aB^P/\rho_m^{P-1}, \quad (2)$$

where ρ_r is the residual resistivity, as before, and $\rho_D(H) = \rho_1 + \rho_d(H)$ is the domain resistivity with ρ_1 being its high-field limit. For present purposes, it will not be necessary to inquire closely into the detailed origin of ρ_D . It is well known experimentally that the low-temperature resistivity of a simple ferromagnet is different in a multidomain state than in a single-domain state. This may be due to

orientation dependence of the normal magnetoresistance¹⁸ within a domain or to scattering at domain boundaries.¹⁹ In either case, strong temperature dependence is not expected. The form of the last term in Eq. (2) is suggested by Kohler's rule where a and P are constants and ρ_m is the resistivity at the minimum.¹⁵ The terms in Eq. (2) were determined by a least-squares-fitting procedure as follows: The data for fields $H > 25$ kOe (i.e., well above technical magnetization) were fitted to $\rho_n + aB^P/\rho_m^{P-1}$, thus determining $\rho_n = \rho_r + \rho_1$, as well as a and P . This result was then subtracted from $\rho(1.2\text{K}, H)$ to yield $\rho_d(H)$, the field-dependent component of $\rho_D(H)$, which was found to be well described by²⁰ $\rho_d(H) = \rho_d(0)e^{-AH}$. In practice, it was found to be convenient to apply this fitting procedure to the corresponding dimensionless form, with $T = 1.2$ K;

$$R^*(T, H)/R_0 = \{R_n + CB^P/[R_m^*(T)]^{P-1} + R_d(H)\}/R_0. \quad (3)$$

The values of the parameters deduced from this nonlinear least-squares fit are given in Table I.

In order to extract the temperature-dependent resistivity, we retain the previously discussed hypothesis that the field-dependent resistivity at $T = 1.2$ K serves as a baseline from which inelastic contributions to ρ may be measured. It must be emphasized that Eq. (3) may be regarded as a quantitative parametrization of this $T = 1.2$ K baseline, and its utility in this respect is independent of the interpretation of the individual components. An estimate of the phonon resistivity at higher temperatures can be obtained if we assume that magnons are fully suppressed by magnetic fields substantially greater than H_m , the field at the minimum of a given isotherm. Then the spin-wave resistivity is essentially zero and the total resistivity is described by Eq. (3) with R_n replaced by $R_n(T) = R_r + R_1 + R_p(T)$. Note that the minimum in the magnetoresistance moves to higher fields as the temperature increases so the experimentally accessible range over which this approach may be used gets smaller. To determine the temperature-dependent parameter $R_n(T)$, and hence the phonon resistivity, it is sufficient to use the previously determined parameters for the temperature-independent background. Following this procedure,

TABLE I. Nonmagnetic resistivity and domain-resistivity parameters (see text).

Crystal orientation	$10^6 \frac{C}{R_0}$	P	$10^4 \frac{R_d(0)}{R_0}$	$10^3 A \text{ (kOe)}^{-1}$
Tb $\langle 10\bar{1}0 \rangle$	129.5 \pm 1	1.161 \pm 0.016	430 \pm 6	456
Ho $\langle 10\bar{1}0 \rangle$	55.88 \pm 0.04	1.40 \pm 0.01	182 \pm 1	655
Ho $\langle 11\bar{2}0 \rangle$	20.18 \pm 0.01	1.567 \pm 0.013	103 \pm 2	456

the spin-wave resistivity is given as that part of the inelastic scattering which can be suppressed by an applied field,

$$R_s(T, H) = R^*(T, H) - R_n(T) - R_d(H) - C_B^P [R_m^*(T)]^{P-1}. \quad (4)$$

To illustrate the results of this analysis, we have plotted $\rho_s(T, H=0)$ for a Ho b -axis crystal as the lower curve in the insert in Fig. 5 so as to compare with the results of the previous method. It should be emphasized that these two methods purposely represent extreme and complementary situations. In the initial approach, taking the phonon resistivity to be described by that of Lu implies that a substantial magnon contribution remains even at rather high fields, while the second approach assumes that 80 kOe is sufficient to suppress essentially all magnon scattering. For this reason, we feel that the two methods yield approximate upper and lower bounds to the true spin-wave resistivity. In this case, Fig. 5 suggests that the average ρ_s is known to within $\pm 20\%$.

On the basis of these results, we conclude that adequate estimates of the contributions to the total resistivity have been obtained and their temperature and field dependences will now be discussed. Detailed results will be given only for the second method of analysis. The parameters describing the field-dependent background (the $T = 1.2$ K isotherm) are given in Table I. In Fig. 6, we give a log-log plot of the phonon resistivity as a function of temperature for the b -axis crystals. The data are seen to be well described by power laws²¹ of the form

$$[R_n(T) - R_n]/R_0 = bT^m. \quad (5)$$

Values of the parameters b and m were determined by a least-squares fit and are given in Table II. These results show that the phonon resistivities of Tb, Ho, and Lu¹⁷ are very similar indeed. Finally, the temperature and field dependence of the spin-wave resistivity deduced via Eq. (4) can be described.

For the Tb b -axis crystal, spin-wave resistivity isotherms are plotted as a function of applied field in Fig. 7 while a log-log plot of the temperature dependence at constant field is given in Fig. 8. The latter shows that the spin-wave resistivity can also be empirically described by a simple power law in the intermediate temperature range,

$$R_s(T, H)/R_0 = aT^n. \quad (6)$$

Values of a and n determined by a least-squares fit are also given in Table II. It may be noted that the exponent n is independent of H at low fields (less than about 20 kOe) but tends to increase at

higher fields. This may be due in part to the "breakdown" of a simple power-law description at high T . However, it should be noted that the intrinsic uncertainties in extracting $\rho(T, H)$ also increase at high fields so that less significance

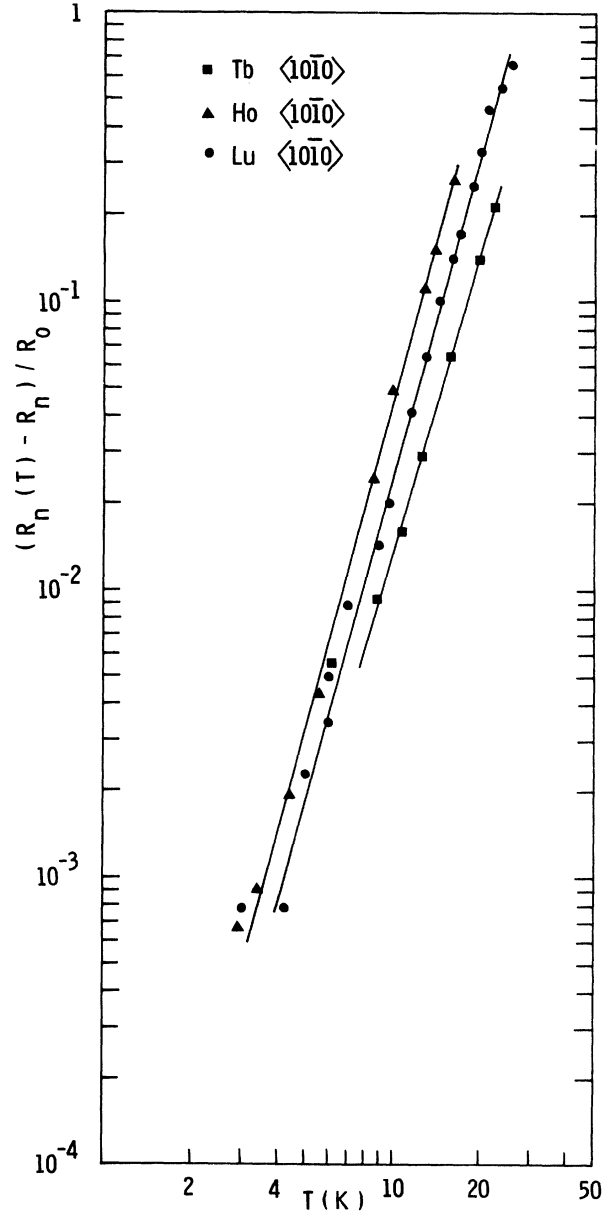


FIG. 6. Variation of the deduced phonon resistivity as a function of temperature in the b -axis crystals of Tb and Ho metals. The normalization constant R_0 is the total resistance at 1.2 K and at $H = 0$; R_n is the field-independent part of the resistance at 1.2 K. For comparison, the resistivity results of nonmagnetic Lu metal (data from Ref. 19) are also shown in the figure, in this case $R_0 = R_n$ is equal to the total resistance at 1.3 K.

TABLE II. Comparison of phonon and spin-wave resistivity parameters.

Sample	Temperature range (K)	$\frac{R_n(T) - R_n}{R_0} = bT^m$		$\frac{R_s(T)}{R_0} = aT^n$	
		$10^6 b$	m	$10^6 a$	n
Tb $\langle 10\bar{1}0 \rangle$	8–23	2.9 ± 0.4	3.7 ± 0.5	0.15 ± 0.03	4.1 ± 0.2
Ho $\langle 10\bar{1}0 \rangle$	3–15	4 ± 0.1	3.7 ± 0.1	2.1 ± 0.1	3.1 ± 0.2
Ho $\langle 11\bar{2}0 \rangle$	3–18	7.5 ± 2	3.7 ± 0.1	2.4 ± 0.8	4.1 ± 0.2
Lu $\langle 10\bar{1}0 \rangle$	4–25	3.6 ± 0.3^a	3.7 ± 0.1^a		

^a Data from Ref. 17.

should be attached to the very-high-field results. For example, a detailed analysis of the Tb a -axis data is not feasible by this method since the minima of the isotherms occur at relatively high fields with the consequence that too few data points are experimentally accessible for $H > H_m$ and the quality of the fits is low.

The spin-wave resistivity isotherms for the b - and a -axis Ho crystals are very similar; a few b -axis isotherms are shown in Fig. 9. At low fields ($H < 5$ kOe), the rapid decrease in ρ_s is attributed to the change in the spin structure of the metal. Thus, the magnetic-field-induced phase transition in this metal decreases the resistivity and does

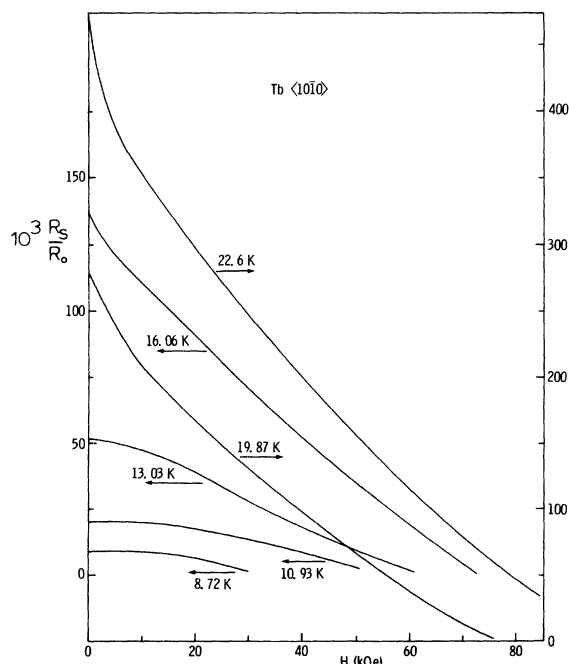


FIG. 7. Deduced spin-wave resistivity isotherms as a function of the applied field for the Tb $\langle 10\bar{1}0 \rangle$ -axis crystal. The error in R_s/R_0 due to uncertainties contributed by the various parameters is about $\pm 6 \times 10^{-4}$ and is temperature independent.

not increase it as suggested by Mackintosh and Spanel.²² At higher fields, the qualitative features of these curves are very similar to those of the Tb b -axis. In Fig. 10, typical spin-wave resistivity isofield curves are shown on a log-log plot as a function of temperature. The values of the parameters a and n [see Eq. (6)] derived from a least-squares fit to the zero-field curve are also given in Table II.

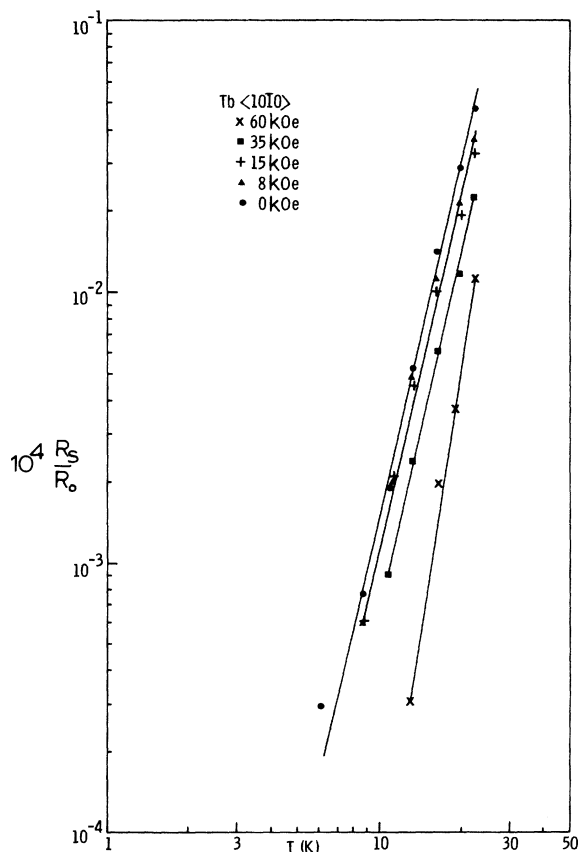


FIG. 8. Deduced spin-wave resistivity isofield data as a function of temperature for the Tb $\langle 10\bar{1}0 \rangle$ -axis crystal. At low fields ($H \leq 20$), the slope is essentially constant but it gradually rises at higher fields.

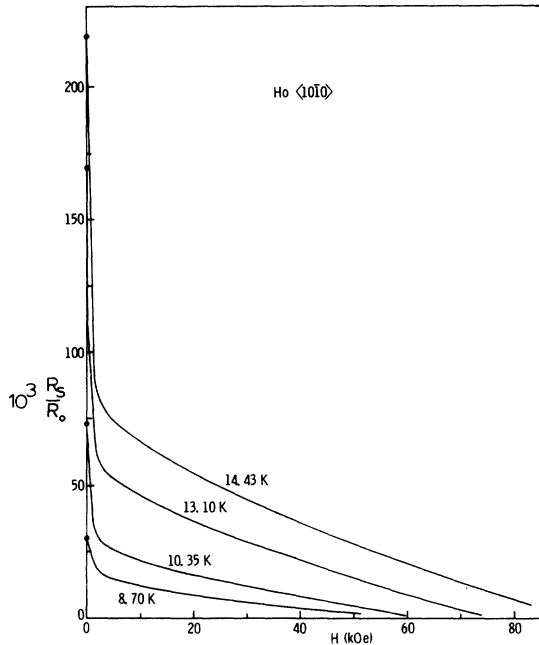


FIG. 9. Deduced spin-wave resistivity isotherms as a function of the applied field for the Ho $\langle 10\bar{1}0 \rangle$ -axis crystal. The error in R_s/R_0 due to uncertainties contributed by the various parameters is about $\pm 4 \times 10^{-4}$.

The results of this analysis and their implications are discussed in the following section.

V. SUMMARY AND DISCUSSION

In Sec. IV, we described a phenomenological method for separating the inelastic phonon and spin-wave resistivity from the measured magnetoresistance. In the temperature range of approximately 4–20 K (see Table II), the phonon resistivity is very well described by a simple power law of the form $\rho_p(T)/\rho_0 = bT^m$. The coefficient b is sample dependent and also depends on the crystallographic direction. It is noteworthy, however, that the exponent m is the same for all samples considered and that this value of $m \approx 3.7$ also described the phonon T dependence of polycrystalline Gd,⁵ and b -axis Lu,¹⁷ crystals. This fact suggests that this power law for $\rho_p(T)$ may be common to all of the heavy-rare-earth metals and increases our confidence in the method of analysis. Note, in particular, that the Bloch T^5 law is not followed. This is not surprising in view of the complex band scheme of the metals and the fact that the many simplifying approximations inherent in the Bloch T^5 law can hardly be valid.

One of the major motivations of this work was the determination of the temperature and field dependence of the spin-wave resistivity. To be spe-

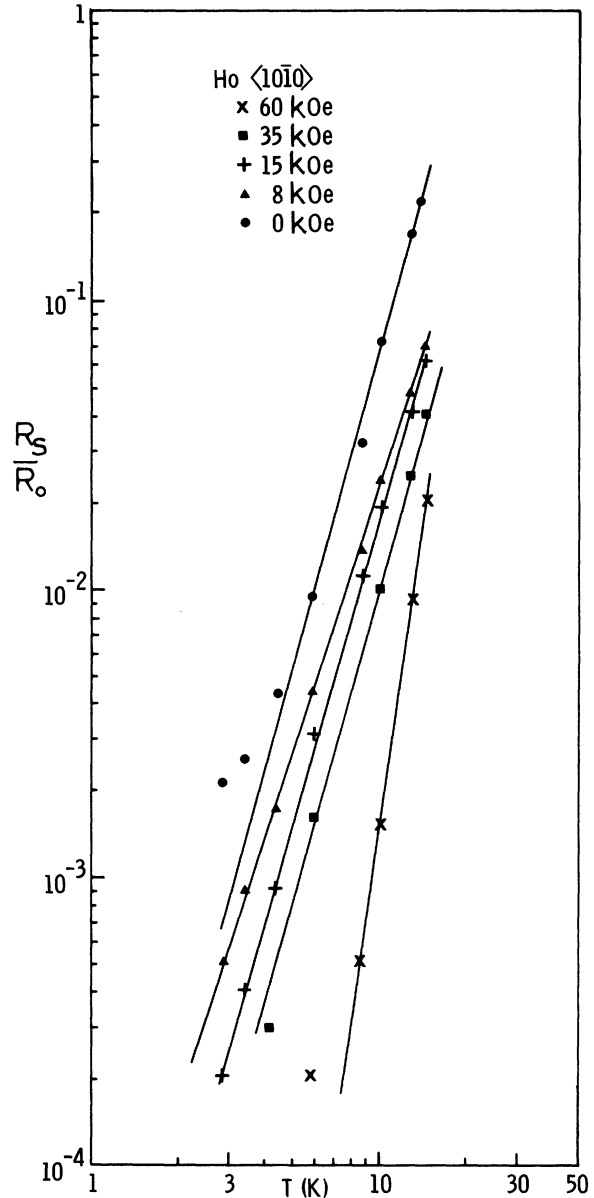


FIG. 10. Deduced spin-wave resistivity isofield data as a function of the temperature for the Ho $\langle 10\bar{1}0 \rangle$ -axis crystal. The slope of the isofield curves gradually rises as field increases.

cific, it has been suggested that the magnon energy gap should be rather directly reflected in the electrical resistivity.⁴ If so, one could exploit the relatively simple and accurate measurements of transport properties to study the temperature and field dependence of $\Delta(T, H)$ and gain thereby information concerning the magnetic anisotropy of the heavy-rare-earth metals. To appreciate this point, suppose that the dispersion law for long-

wavelength (acoustical) magnons may be approximated by²³

$$\epsilon(\vec{q}) = \Delta + D\vec{q}^2.$$

In the absence of Δ , the spontaneous magnetization follows the Bloch $T^{3/2}$ law, $M(0) - M(T) \propto T^{3/2}$. For $\Delta \neq 0$, Niirha²⁴ showed that this should be replaced by $M(0) - M(T) \propto T^{3/2}e^{-T_0/T}$, where $T_0 = \Delta(T=0, H=0)/k_B$ (the constant of proportionality is also altered). The corresponding spin-wave resistivity for $\Delta=0$ was shown by Mannari²⁵ and Kasuya²⁶ to be given by $\rho_S(T) \propto T^2$. Based on the analogy with the spontaneous magnetization, Macintosh⁴ suggested that this result should be replaced, for $\Delta \neq 0$, by

$$\rho_S(T, H=0) \propto T^2 e^{-T_0/T}. \quad (7)$$

If so, this relatively strong T dependence could be detectable²⁷ and the field dependence of $\Delta(T, H)$ could also be studied. However, the analysis of Sec. IV shows that the spin-wave resistivity is describable by a simple power law in the approximate temperature range 4–20 K (see Table II). Clearly, the range of validity of Eq. (7) should be established more precisely. To generate some feeling for this question, we have made a simple-model calculation of $\rho_S(T)$ in a one-magnon approximation. With the usual simplifying approximations,^{25,26} such as describing the conduction electrons by spin-split spherical bands, treating electron-magnon scattering in the Born approximation, neglecting umklapp processes, and replacing the exchange interaction $J_{sf}(\vec{q})$ by a constant pseudopotential, a straightforward treatment of the weak inelastic scattering leads to

$$\rho_S(T)/\rho_{dis} = [8/(J+1)]I(T), \quad (8)$$

where

$$I(T) = (16\pi k_F^4)^{-1} \sum_{\lambda} \int_{q_0}^{2k_F} d^3q q \beta \epsilon_q^\lambda n_{q\lambda} (1 + n_{q\lambda}). \quad (9)$$

In Eq. (9), q_0 is the minimum wave vector for a spin-flip transition, $\beta = (k_B T)^{-1}$, ϵ_q^λ are the magnon dispersion laws (acoustical and optical in hcp crystals), and $n_{q\lambda}$ is the Bose-Einstein distribution function. In the low-temperature limit, the optical branch can be neglected and Eq. (9) can be expanded in powers of the small parameter $e^{-T_0/T}$. The lowest-order result is

$$I_1(T) = 2(k_B T_0 / 4Dk_F^2)^2 \times [\phi + (1 + \phi)T/T_0 + 2(T/T_0)^2] e^{-T_0/T}. \quad (10)$$

In practice, $\phi \approx Dq_0^2/k_B T_0 \sim 10^{-2}$ and can be neglected. It is clear, in any case, that Eq. (7) does not correctly represent the low-temperature behavior of $\rho_S(T)$. The presence of the energy gap compli-

cates somewhat the low-temperature expansion and introduces additional terms. Moreover, it can be shown that further terms of order $T^2 e^{-T_0/T}$ are contributed by quadratic terms in the expan-

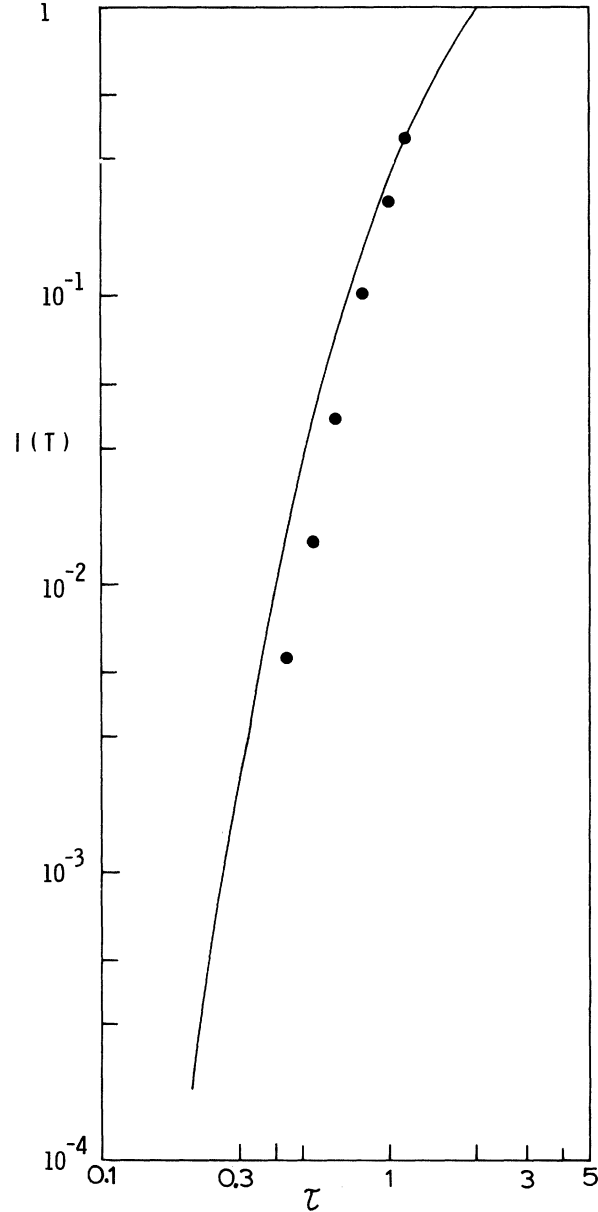


FIG. 11. Calculated spin-wave resistivity integral $I(T)$ [which is directly proportional to $\rho_S(T)/\rho_{dis}$, see Sec. V] as a function of $\tau = T/T_0$ for the Tb b -axis crystal. The dots represent the experimentally deduced temperature dependence of the spin-wave resistivity for $T_0 = 20$ K. The data points have been multiplied by a constant ($= 7.4$) so that they are normalized to the calculated curve at 22.6 K. Since the experimental and theoretical results involved different normalization constants initially, they can be shifted vertically for comparison of the temperature dependence.

sion of $J_{sf}(\vec{q})$ and by quadratic terms in the magnon dispersion relation. Details of the complete low-temperature expansion will not be given as its usefulness is limited to temperatures such that $e^{-T_0/T} \ll 1$. In this range, however, the resistivity is dominated by the residual resistivity and sufficiently accurate estimates of ρ_S are very difficult to obtain. For this reason, the prospect of obtaining information about the energy gap from ρ_S appears feasible only if $\Delta(T, H)$ is reflected in ρ_S in a characteristic way in the *intermediate* temperature range (say, $0.2 \leq T/T_0 \leq 1$).

At intermediate temperatures, Eq. (9) can no longer be evaluated analytically in closed form in terms of standard functions so the integration was performed numerically. For simplicity, the energy of the optical branch was taken to be a constant, ϵ_{opt} , and the acoustical branch was described by

$$\epsilon_{ac}(q) = \Delta + Dq^2(1 - q^2/2q_D^2), \quad (11)$$

where q_D is the Debye wave number, in an attempt to include some of the structure at larger q . Equation (9) was evaluated for a range of values of temperature and model parameters. Representa-

tive numerical results²⁸ are given as a log-log plot in Fig. 11 as a function of $\tau = T/T_0$. For comparison, the experimental results for a Tb *b*-axis crystal (with $T_0 = 20$ K) are also given. The following points should be noted. The calculated results show no sharp structure and increase monotonically with temperature, even in the vicinity of $T = T_0$. Also, if fitted to a power law, the calculated and experimentally determined $\rho_S(T)$ have rather similar temperature dependences for $T < T_0$. We conclude that, even in this simple and favorable model, the energy gap is not reflected in the spin-wave resistivity in an obviously transparent way. We conclude that attempts to extract $\Delta(T, H)$ from the measured ρ_S of real systems appear to be far less promising than heretofore suggested,²⁹ particularly in the absence of a clearly adequate theory of simple transport properties in these complex systems which might assist in the interpretation.

ACKNOWLEDGMENTS

We wish to thank B. Paton for the use of his superconducting magnet and D. A. Goodings for discussion.

*Supported in part by the National Research Council of Canada.

¹T. Kasuya, Prog. Theor. Phys. **16**, 58 (1956).

²P. G. de Gennes and J. Friedel, J. Phys. Chem. Solids **4**, 71 (1958).

³S. Legvold, Phys. Rev. B **3**, 1640 (1971).

⁴A. R. Mackintosh, Phys. Lett. **4**, 140 (1963).

⁵B. Lüthi and H. Rohrer, Solid State Commun. **3**, 257 (1965).

⁶Very-low-temperature experiments (down to 60 mK) on some of the samples revealed that in the Tb samples the resistivity was not residual below 1.2 K but that it was essentially residual for Ho. [See D. A. Tindall and M. H. Jericho, J. Phys. F **5**, 1359 (1975).] The cause for the unusual behavior in Tb was traced to impurity effects with oxygen possibly playing a significant role. The effect was, however essentially magnetic field independent, and our magnetoresistance results in Tb above 1.2 K should not be affected significantly by these impurities.

⁷R. L. Singh and M. H. Jericho (unpublished).

⁸In addition to modifying various scattering mechanisms, the magnetic field also produces changes in the sample dimensions due to magnetostriction effects. The sample shape factor $F = (\text{cross section area}) / (\text{length of specimen between potential probes})$ is then field dependent. Since the measured current ratio I_r/I_S is proportional to the sample resistance $R(H)$, the corrected magnetoresistance which is given by $R^*(H)/R(0) = [(I_r/I_S)_H / (I_r/I_S)_0] [F(H)/F(0)]$ can be directly compared to the corresponding resistivity ratio $\rho(H)/\rho(0)$. In Tb, maximum strains of the order of 3×10^{-3} along the *a*-

and *b*-axis crystal directions have been reported [J. J. Rhyne and S. Legvold, Phys. Rev. **138**, A507 (1965); and U.S. AEC report No. IS-T-21 (1965) (unpublished)]. These data were used to calculate the shape factor for our Tb *b*-axis crystals. For $H > 10$ kOe, $F(H)/F(0) \approx 0.9932$ and is essentially constant in the present temperature range. This correction slightly reduces the resistance in this case and at 1.22 K the depth of the minimum changes from 2.48% to 3.14%. In the case of Ho *a*- and *b*-axis crystals, the data were not corrected for magnetostriction since the effect turned out to be negligible. Using the results of S. Legvold, J. Alstad, and J. J. Rhyne [Phys. Rev. Lett. **10**, 509 (1963)], we estimated a change in resistance of only 0.02% for the *b*-axis Ho crystal.

⁹D. E. Hegland, S. Legvold, and F. H. Spedding, Phys. Rev. **131**, 158 (1963).

¹⁰D. L. Strandburg, Ph.D. thesis (Iowa State University of Science and Technology, 1961) (unpublished).

¹¹See, for example, the review by T. R. McGuire and R. I. Potter, Trans. Magn. **11**, 1018 (1975). These authors discuss the role played by domain effects anisotropy, sample purity, etc., for 3*d*-series metals and alloys.

¹²M. Kohler, Ann. Phys. **32**, 211 (1938). Kohler plots are discussed by J. M. Ziman [in *Electrons and Phonons* (Clarendon, Oxford, 1960)] for nonmagnetic metals and by T. R. McGuire and R. I. Potter in Ref. 11 for 3*d*-transition-series ferromagnets.

¹³A. C. Ehrlich, R. Huguenin, and D. Rivier, J. Phys. Chem. Solids **28**, 253 (1967).

¹⁴F. C. Schewerer and J. Silcox, Phys. Rev. Lett. **20**,

101 (1968).

- ¹⁵It should be emphasized that it is precisely the feature of relatively high residual resistivity which renders the following analysis insensitive to the choice of $\rho(T,0)$ in the case of the heavy-rare-earth metals. This is in striking contrast to the case of the relatively purer 3rd-transition metals (see Refs. 11, 13, and 14) where application of Kohler's rule is more delicate. In the second method of analysis, where a detailed parametrization is given for the field-dependent background, $\rho(T,0)$ has been replaced by the resistivity at the minimum of the isotherm. For the above reason, the results are insensitive to the precise choice (within reason) of the low-field limit.
- ¹⁶K. A. Gschneidner, Jr., *The Rare Earth Alloys* (Van Nostrand, Princeton, N.J., 1961).
- ¹⁷D. W. Boys, Ph.D. thesis (Iowa State University of Science and Technology, 1968) (unpublished).
- ¹⁸L. Berger and A. R. De Vrooman, *J. Appl. Phys.* **36**, 2777 (1965).
- ¹⁹A. I. Sudovtsov and E. E. Semenenko, *Zh. Eksp. Teor. Fiz.* **35**, 305 (1958) [*Sov. Phys.-JETP* **8**, 211 (1959)]; E. E. Semenenko and A. I. Sudovtsov, *Zh. Eksp. Teor. Fiz.* **47**, 486 (1964) [*Sov. Phys.-JETP* **20**, 323 (1965)].
- ²⁰The exponential dependence of $\rho_d(H)$ on the applied field is suggestive of a Boltzmann-like factor in which the response of the multidomain specimen to applied magnetic fields is opposed by intrinsic magnetic anisotropy. Technical saturation of magnetization occurs for $H \gg H_{\text{anis}} = 1/A$.
- ²¹In the case of the Tb *b*-axis crystal, there are deviations from a simple power law for $T \lesssim$ a few K, believed to be due to impurities (see Ref. 6). This additional source of resistivity precludes determination of $\rho_p(T)$ at the lower temperatures. Consequently, the power-law fit, Eq. (5), of the phonon resistivity was restricted to the range $T > 10$ K in this case.
- ²²A. R. Mackintosh and L. E. Spinel, *Solid State Commun.* **2**, 383 (1964).
- ²³Owing to the characteristic magnetic anisotropy of the heavy-rare-earth ferromagnets, the energy of a long-wavelength "acoustical" magnon is not zero; $\epsilon(\vec{q}) \rightarrow \Delta = 0$ as $\vec{q} \rightarrow \vec{0}$. A recent review of the role played by the magnon energy gap Δ in various properties of the rare-earth metals has been given by A. R. Mackintosh and H. B. Møller [in *Magnetic Properties of Rare Earth Metals* edited by R. J. Elliott (Plenum, New York, 1972)].
- ²⁴K. Niirha, *Phys. Rev.* **117**, 129 (1960).
- ²⁵I. Mannari, *Prog. Theor. Phys.* **22**, 335 (1959); **26**, 51 (1961).
- ²⁶T. Kasuya, *Prog. Theor. Phys.* **22**, 227 (1959).
- ²⁷Recently, N. H. Sze, K. V. Rao, and G. T. Meaden [*J. Low Temp. Phys.* **1**, 563 (1969)] reported a small hump (about 2% relative to the background) in the electrical resistivity of a Tb *c*-axis crystal at a temperature about 21.5 K and attributed it to the energy gap. However, it is obvious from Eq. (7) as well as from more detailed treatment (see following discussion) that there is no theoretical reason to expect a $\vec{q} = \vec{0}$ gap in the magnon spectrum to give rise to a local maximum in ρ_s around $T = T_0$. Moreover, in an attempt to clarify this question, we made precise measurements on *a*-, *b*-, and *c*-axis Tb crystals cut from the same stock as the sample used by Sze *et al.* We found the resistivity to increase quite gradually and monotonically, even for $T \approx T_0$, in all cases and there was no indication of the anomalous behavior reported by the above authors.
- ²⁸The calculated results in Fig. 11 were obtained for $Dq_B^2/k_B T_0 = 5$, $\epsilon_{\text{opt}}/k_B T_0 = 4$, $q_0/k_F = 0.1$, and $2k_F/q_D = 1$. The parameters were chosen to give a crude representation of the average magnon spectrum determined experimentally for Tb [J. Jensen, J. H. Houmann, and H. Hjerrum Møller, *Phys. Rev. B* **12**, 303 (1975)].
- ²⁹See Ref. 27 and Sec. 5.7.4 of Ref. 23.